

A Simple Stochastic Model for El Niño with Westerly Wind Bursts: Supplementary Information

Sulian Thual ⁽¹⁾, Andrew J. Majda ⁽¹⁾, Nan Chen⁽¹⁾, Samuel N. Stechmann ⁽²⁾

(1) Department of Mathematics, and Center for Atmosphere Ocean Science, Courant Institute of Mathematical Sciences, New York University, 251 Mercer Street, New York, NY 10012 USA

(2) Department of Mathematics, and Department of Atmospheric and Oceanic Sciences, University of Wisconsin - Madison, 480 Lincoln Drive, Madison, WI 53706 USA

The supplementary information is organized as follows. In Section 1 we detail the asymptotic expansion used to derive the ENSO model at the interannual timescale. In Section 2 we detail the model's meridional truncation. In Section 3 we provide additional theoretical details on the two-state Markov jump process. In Section 4 we detail the algorithm for solving the model. In Section 5 we present linear solutions of the model.

1 Asymptotic Expansion

This section provides details on the derivation of the ENSO model used in the article.

We start with the derivation from a more complete model that consists of the skeleton model in the atmosphere (1) coupled to a shallow water ocean in the long-wave approximation and a SST budget (2). Intraseasonal timescale t is used for the atmosphere and interannual timescale τ for the ocean and SST, with $\tau = \epsilon t$ where ϵ is the Froude number. The complete starting model is as follows:

Interannual atmosphere model

$$\begin{aligned}
 (\epsilon\partial_\tau + \epsilon d_A)u - yv - \partial_x\theta &= 0 \\
 yu - \partial_y\theta &= 0 \\
 (\epsilon\partial_\tau + \epsilon d_A)\theta - (\partial_x u + \partial_y v) &= \bar{H}a - s^\theta \\
 (\epsilon\partial_\tau + \epsilon d_A)q + \bar{Q}(\partial_x u + \partial_y v) &= -\bar{H}a + s^q + E_q \\
 \epsilon\partial_\tau a &= \Gamma qa
 \end{aligned} \tag{1}$$

Interannual ocean model

$$\begin{aligned}
 (\epsilon\partial_\tau + \epsilon^2 d_O)U - c_1\epsilon YV + c_1\epsilon\partial_x H &= c_1\epsilon\tau_x \\
 YU + \partial_Y H &= \sqrt{c_1\epsilon}\delta^2\tau_y \\
 (\epsilon\partial_\tau + \epsilon^2 d_O)H + c_1\epsilon(\partial_x U + \partial_Y V) &= 0
 \end{aligned} \tag{2}$$

Interannual SST model

$$\epsilon\partial_\tau T = -c_1\epsilon\zeta E_q + c_1\epsilon\eta H - c_1\epsilon\alpha(a - \bar{a}) \tag{3}$$

Couplings

$$\begin{aligned}
 E_q &= (q_c \exp(q_e(T + \bar{T})) - q_c \exp(q_e(\bar{T})) - \beta_q q) / \tau_q \\
 (\tau_x, \tau_y) &= \gamma(u, v)
 \end{aligned} \tag{4}$$

In the model, the atmosphere extends over the entire equatorial belt $0 \leq x \leq L_A$, while the ocean Pacific extends from $0 \leq x \leq L_O$, with $L_O < L_A$. There are periodic boundary conditions in the atmosphere $u(0, y, t) = u(L_A, y, t)$, etc and reflection boundary conditions in the ocean $\int_{-\infty}^{+\infty} U(0, Y, t) dY = 0$ and $U(L_O, Y, t) = 0$ (see e.g. 3, chapter 4). Table S1 provides the definition

and units of all model variables. Table S3 provides the definition and values of all model parameters, while Table S2 provides the definition and value of additional parameters used for rescaling.

In order to obtain the ENSO model in its final form, we consider the first order of an asymptotic expansion of the above system in orders of powers of ϵ , with the generic form $\underline{U} = \sum_{n=1}^N \underline{U}_n \epsilon^n + o(\epsilon^N)$, where $\underline{U} = \{u, v, \theta, a, U, V, H, T\}$. This asymptotic expansion is performed on the interannual timescale τ only, while fluctuations on the intraseasonal timescale t are omitted. The resulting system reads:

Interannual atmosphere model

$$\begin{aligned}
-yv - \partial_x \theta &= 0 \\
yu - \partial_y \theta &= 0 \\
-(\partial_x u + \partial_y v) &= \overline{H}a - s^\theta \\
\overline{Q}(\partial_x u + \partial_y v) &= -\overline{H}a + s^q + E_q \\
0 &= q
\end{aligned} \tag{5}$$

Interannual ocean model

$$\begin{aligned}
\partial_\tau U - c_1 YV + c_1 \partial_x H &= c_1 \tau_x \\
YU + \partial_Y H &= 0 \\
\partial_\tau H + c_1(\partial_x U + \partial_Y V) &= 0
\end{aligned} \tag{6}$$

Interannual SST model

$$\partial_\tau T = -c_1 \zeta E_q + c_1 \eta H - c_1 \alpha (a - \bar{a}) \tag{7}$$

Couplings

$$\begin{aligned}
E_q &= (q_c \exp(q_e(T + \overline{T})) - q_c \exp(q_e(\overline{T})) - \beta_q q) / \tau_q \\
\tau_x &= \gamma u
\end{aligned} \tag{8}$$

Finally, several simplifications are considered in order to obtain the model in its final form. First, we assume balanced external sources of heating and moistening $s^\theta = s^q$ in the atmosphere, and combine the rows from equation (5) to eliminate the prognostic variable $\overline{H}a = (E_q + s^q - \overline{Q}s^\theta)/(1 - \overline{Q})$. Second, we linearize latent heating anomalies as $E_q = \alpha_q T$, which is a reasonable approximation for the planetary and interannual timescales under consideration here. Third, we

absorb the cloud radiative feedback term $\alpha(a - \bar{a})$ of the SST budget that has the same form as the dissipation term $-\zeta E_q$.

With the above modifications and with the addition of atmospheric noise, we obtain the model in final form in the present article. In addition to this, when computing solutions the model is truncated meridionally to the first parabolic cylinder functions of the ocean and atmosphere, which is detailed in the next section.

Variable	unit	unit value
x zonal axis	$[y]/\delta$	15000km
y meridional axis atmosphere	$\sqrt{c_A/\beta}$	1500km
Y meridional axis ocean	$\sqrt{c_O/\beta}$	330km
t time axis intraseasonal	$1/\delta\sqrt{c_A\beta}$	3.3 days
τ time axis interannual	$[t]/\epsilon$	33 days
u zonal wind speed anomalies	δc_A	5 ms^{-1}
v meridional wind speed anomalies	$\delta[u]$	0.5 ms^{-1}
θ potential temperature anomalies	15 δ	1.5K
q low-level moisture anomalies	$[\theta]$	1.5K
a envelope of synoptic convective activity	1	
$\bar{H}a$ convective heating/drying	$[\theta]/[t]$	0.45 $K.day^{-1}$
E_q latent heating anomalies	$[\theta]/[t]$	0.45 $K.day^{-1}$
T sea surface temperature anomalies	$[\theta]$	1.5K
U zonal current speed anomalies	$c_O\delta_O$	0.25 ms^{-1}
V zonal current speed anomalies	$\delta\sqrt{c}[U]$	0.56 cms^{-1}
H thermocline depth anomalies	$H_O\delta_O$	20.8 m
τ_x zonal wind stress anomalies	$\delta\sqrt{\beta/c_A}H_O\rho_Oc_O^2\delta_O$	0.00879 $N.m^{-2}$
τ_y meridional wind stress anomalies	$[\tau_x]$	0.00879 $N.m^{-2}$

Table S1: Model variables definitions and units.

Rescaling parameter	value
ϵ Froude number	0.1
δ long-wave scaling	0.1
δ_O arbitrary constant	0.1
c_A atmosphere phase speed	50 ms^{-1}
c_O ocean phase speed	$\sqrt{g'H_O} = 2.5 ms^{-1}$
c ratio of ocean/atmosphere phase speed	$c_O/c_A = 0.05$
c_1 modified ratio of phase speed	$c/\epsilon = 0.5$
β beta-plane parameter	$2.28 \cdot 10^{-11} m^{-1} s^{-1}$
g' (reduced gravity)	0.03 ms^{-2}
H_O mean thermocline depth	208 m
ρ_O ocean density	1000 $kg.m^{-3}$

Table S2: Model parameters used for rescaling.

Parameter	nondimensional value
c ratio of ocean/atmosphere phase speed	0.05
ϵ Froude number	0.1
$c_1 = c/\epsilon$	0.5
χ_A meridional projection coefficient atmosphere	0.31
χ_O meridional projection coefficient ocean	1.38
L_A equatorial belt length	8/3
L_O equatorial Pacific length	1.2
\overline{H} convective heating rate factor	22
\overline{Q} mean vertical moisture gradient	0.9
s^θ external source of cooling	2.2
s^q external source of moistening	2.2
α_q latent heating factor	$\alpha_q = q_c q_e \exp(q_e \overline{T}) / \tau_q$
q_c latent heating multiplier coefficient	7
q_e latent heating exponential coefficient	0.093
τ_q latent heating adjustment rate	15
\overline{T} mean SST	16.6
γ wind stress coefficient	6.53
r_W western boundary reflection coefficient	0.5
r_E eastern boundary reflection coefficient	1
ζ latent heating exchange coefficient	8.7
η profile of thermocline feedback	$\eta(x) = 1.5 + (0.5 \tanh(7.5(x - L_O/2)))$
d_p wind burst damping	3.4
s_p wind burst zonal structure	$s_p(x) = \exp(-45(x - L_O/4)^2)$
σ_{p0} wind burst source of quiescent state	0.2
σ_{p1} wind burst source of active state	2.6
μ_{01} transition rate quiescent to active state	$\mu_{01} = 0.125(\tanh(2T_w) + 1)$
μ_{10} transition rate active to quiescent state	$\mu_{10} = 0.25(1 - \tanh(2T_w))$

Table S3: Model parameter definitions and values.

2 Meridional Truncation

In order to compute the solutions of the ENSO model, we consider the model in its simplest form truncated meridionally to the first parabolic cylinder functions.

For this, we consider different parabolic cylinder functions in the ocean and atmosphere, that are shown in Figure S4. The first atmospheric parabolic cylinder functions read $\phi_0(y) = (\pi)^{-1/4} \exp(-y^2/2)$, $\phi_2 = (4\pi)^{-1/4} (2y^2 - 1) \exp(-y^2/2)$, while the ocean parabolic cylinder functions read $\psi_m(Y)$, identical to the previous expression except depending here on the Y axis. If we express both the ocean and atmosphere systems as a function of the axis y , we must use instead

$$\psi_m(y) = \phi_m(Y) \text{ where } Y = y/\sqrt{c}.$$

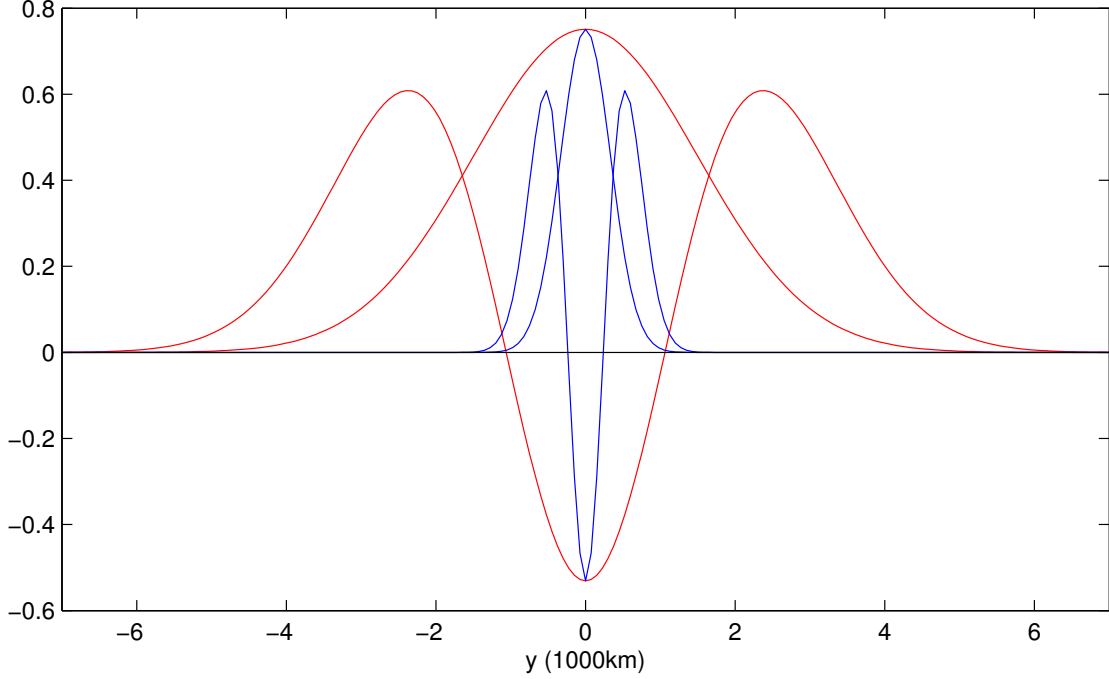


Figure S4: Meridional profiles of atmosphere parabolic cylinder functions ϕ_0 , ϕ_2 (red) and ocean parabolic cylinder functions ψ_0 , ψ_2 (blue), as a function of meridional position y (1000km).

The parabolic cylinder functions in the ocean and atmosphere differ by their meridional extent, or Rossby radius. Choosing an identical meridional basis in the ocean and atmosphere would be more rigorous from a mathematical viewpoint: however, when coupling the ocean and atmosphere, a large number of meridional modes would be necessary, which is avoided here (4). For instance, as shown below here only four equatorial waves (K_A , R_A , K_O , R_O) describe the atmosphere and ocean coupled dynamics, which keeps the model low-dimensional for simplicity. In order to couple the ocean and atmosphere, projection coefficients are introduced that reads $\chi_A = \int_{-\infty}^{+\infty} \phi_0(y)\phi_0(y/\sqrt{c})dy$ and $\chi_O = \int_{-\infty}^{+\infty} \psi_0(Y)\psi_0(\sqrt{c}Y)dY$.

In the atmosphere we assume a truncation of moisture, activity and external sources to the first parabolic cylinder function ϕ_0 , $\{a, q, s^\theta, s^q\} = \{a, q, s^\theta, s^q\}\phi_0(y)$ (with a slight abuse of notations). This is known to excite only the Kelvin and first Rossby atmospheric equatorial waves, of amplitude K_A and R_A . In the ocean, we assume a truncation of zonal wind stress forcing to ψ_0 , $\tau_x = \tau_x\psi_0$. This is known to excite only the the Kelvin and first Rossby atmospheric oceanic waves, of

amplitude K_O and R_O . Similarly, for the SST model we assume a truncation $\psi_0, T = T\psi_0$. The ENSO model truncated meridionally reads:

Interannual atmosphere model

$$\begin{aligned}
\partial_x K_A &= -\chi_A E_q (2 - 2\bar{Q})^{-1} \\
-\partial_x R_A/3 &= -\chi_A E_q (3 - 3\bar{Q})^{-1} \\
K_A(0, \tau) &= K_A(L_A, \tau) \\
R_A(0, \tau) &= R_A(L_A, \tau)
\end{aligned} \tag{9}$$

Interannual ocean model

$$\begin{aligned}
\partial_\tau K_O + c_1 \partial_x K_O &= \chi_O c_1 \tau_x / 2 \\
\partial_\tau R_O - (c_1/3) \partial_x R_O &= -\chi_O c_1 \tau_x / 3 \\
K_O(0, t) &= r_W R_O(0, t) \\
R_O(L_O, t) &= r_E K_O(L_O, t)
\end{aligned} \tag{10}$$

Interannual SST model

$$\partial_\tau T / c_1 = -\zeta E_q + \eta(K_O + R_O) \tag{11}$$

Couplings

$$\begin{aligned}
E_q &= \alpha_q T \\
\tau_x &= \gamma(K_A - R_A)
\end{aligned} \tag{12}$$

The reconstructed variables reads:

$$\begin{aligned}
u &= (K_A - R_A)\phi_0 + (R_A/\sqrt{2})\phi_2 \\
\theta &= -(K_A + R_A)\phi_0 - (R_A/\sqrt{2})\phi_2 \\
U &= (K_O - R_O)\psi_0 + (R_O/\sqrt{2})\psi_2 \\
H &= (K_O + R_O)\psi_0 + (R_O/\sqrt{2})\psi_2
\end{aligned} \tag{13}$$

The absence of dissipation in the atmosphere imposes a peculiar solvability condition of a zero

equatorial zonal mean of latent heating forcing (5, 6). This reads:

$$\frac{1}{L_A} \int_0^{L_A} E_q dx = 0 \quad (14)$$

This solvability condition is accounted for when solving equation (9) of the above system.

3 Two-state Markov jump process

This section aims at providing a brief theoretical discussion about the two-state Markov jump process and the intuition of adopting this stochastic parameterization in the ENSO model.

3.1 A brief theoretical discussion about two-state Markov jump process

Suppose a stochastic process X_t can take only one of the two values corresponding to the two states (7),

$$X_t = \begin{cases} s_0 & \text{for state 0} \\ s_1 & \text{for state 1} \end{cases} \quad (15)$$

where the subscript t of X_t represents time and those 0 and 1 of s represent the two states. The process remains in one state before it changes to another at some random time t . We consider a process with Markov property

$$P(X_t = s_i | X_{s \leq r}) = P(X_t = s_i | X_r) \quad (16)$$

and time-homogeneity

$$P(X_t = s_i | X_s = s_j) = P(X_{t-s} = s_i | X_0 = s_j) \quad (17)$$

where $i, j \in \{0, 1\}$. Due to these two properties the process is fully determined by the transition probabilities $P(X_t = s_i | X_0 = s_j)$. Next, we define μ_{01} and μ_{10} as the transition rates from state 0

to state 1 and from state 1 to 0, respectively. These two rates define the following local transition probabilities for small Δt :

$$\begin{aligned}
P(X_{t+\Delta t} = s_1 | X_t = s_0) &= \mu_{01}\Delta t + o(\Delta t) \\
P(X_{t+\Delta t} = s_0 | X_t = s_1) &= \mu_{10}\Delta t + o(\Delta t) \\
P(X_{t+\Delta t} = s_0 | X_t = s_0) &= 1 - \mu_{01}\Delta t + o(\Delta t) \\
P(X_{t+\Delta t} = s_1 | X_t = s_1) &= 1 - \mu_{10}\Delta t + o(\Delta t)
\end{aligned} \tag{18}$$

where $o(\Delta t)$ denotes a function smaller than Δt , i.e. $o(\Delta t)/\Delta t \rightarrow 0$ as $\Delta t \rightarrow 0$.

The transition probability from state 0 to state 1 is $p_{01}(t) = P(X(t) = s_1 | X(0) = s_0)$, which can be written down explicitly,

$$p_{t+\Delta t}(s_0, s_1) = p_t(s_0, s_1)p_{\Delta t}(s_1, s_1) + p_t(s_0, s_0)p_{\Delta t}(s_0, s_1) \tag{19}$$

or alternatively

$$p_{t+\Delta t}(s_0, s_1) = p_t(s_0, s_1)(1 - \mu_{10}\Delta t) + p_t(s_0, s_0)\mu_{10}\Delta t + o(\Delta t). \tag{20}$$

Regrouping terms lead to

$$\frac{p_{t+\Delta t}(s_0, s_1) - p_t(s_0, s_1)}{\Delta t} = -\mu_{10}p_t(s_0, s_1) + \mu_{01}p_t(s_0, s_0) + o(1). \tag{21}$$

In the limit $\Delta t \rightarrow 0$, the following differential equation is obtained:

$$\partial_t p_t(s_0, s_1) = -\mu_{10}p_t(s_0, s_1) + \mu_{01}p_t(s_0, s_0). \tag{22}$$

The equations for all other transition probabilities can be obtained in a similar way. Combine the transition probabilities into the transition probability matrix

$$P_t = \begin{pmatrix} p_t(s_0, s_0) & p_t(s_0, s_1) \\ p_t(s_1, s_0) & p_t(s_1, s_1) \end{pmatrix} \tag{23}$$

Then the differential equation for the matrix P_t is given by

$$\frac{\partial P_t}{\partial t} = P_t A, \quad (24)$$

where the matrix A has the rates of change from one state to another

$$A = \begin{pmatrix} -\mu_{01} & \mu_{01} \\ \mu_{10} & -\mu_{10} \end{pmatrix}. \quad (25)$$

3.2 Application to the wind burst amplitude a_p .

Recall the governing wind burst amplitude a_p ,

$$\frac{da_p}{d\tau} = -d_p a_p + \sigma_p(T_W) \dot{W}(t). \quad (26)$$

The noise coefficient $\sigma_p(T_W)$, that depends on SST anomalies in the western Pacific T_W , is modeled by a two-state Markov jump process as described above. Depending on T_W , $\sigma_p(T_W)$ switches between a quiescent state (of low energy) and an active state (of high energy):

$$\sigma_p(T_W) = \begin{cases} \sigma_{p0} = 0.2 \text{ for state 0 (quiescent)} \\ \sigma_{p1} = 2.6 \text{ for state 1 (active)} \end{cases} \quad (27)$$

Due to the fact that an increase of the SST in the western Pacific leads to an enhanced wind burst activity, the active state corresponds to the instance when the western Pacific SST is high ($T_W \geq 0$). On the other hand, since no strong westerly wind burst is observed with a reduced SST in the western Pacific, a negative anomaly $T_W \leq 0$ is linked with the quiescent state. Given these physical intuitions, the following transition rates are used:

$$\begin{aligned} \text{State 1 to 0: } \mu_{10} &= \frac{1}{4}(1 - \tanh(2T_w)) \\ \text{State 0 to 1: } \mu_{01} &= \frac{1}{8}(\tanh(2T_w) + 1) \end{aligned} \quad (28)$$

Note that we can add complexity and alternatively consider a three-state Markov jump process

to describe the wind burst activity in the model. Despite slightly more natural transitions between El Niño and La Niña events due to the introduction of an intermediary state, the results are not found to be significantly different from the ones with the above two-state Markov jump process (not shown).

4 Numerical Algorithm for the Model

This section describes the numerical solution procedure for the ENSO model. The model is spatially discretized on the grid $i = 1, \dots, n_O$ in the ocean ($n_O = 28$), and $i = 1, \dots, n_A$ ($n_A = 64$) in the atmosphere, which reads $T(x_i) = T_i$, etc with $x_i = i\Delta x$ and $\Delta x = 625 \text{ km}$. The ocean derivatives are discretized using upwind schemes depending on the direction of propagation, $[\partial_x K_O]_i = (K_{O_i} - K_{O_{i-1}})/\Delta x$, $[\partial_x R_O]_i = (R_{O_{i+1}} - R_{O_i})/\Delta x$, with reflection boundary conditions accounted for as $[\partial_x K_O]_1 = (K_{O_1} - r_w R_{O_1})/\Delta x$ and $[\partial_x R_O]_{n_O} = (r_E K_{O_{n_O}} - R_{O_{n_O}})/\Delta x$.

The atmospheric response to latent heating anomalies is computed as follows on the spatial grid:

$$d_A W_{A_i} + \frac{(W_{A_{i+1}} - W_{A_i})}{\Delta x} = \frac{-3\chi_A}{2(1 - \bar{Q})} \left(E_{q_i} - \sum_{i=1}^{n_A} E_{q_i} \frac{\Delta x}{L_A} \right) \quad (29)$$

where $K_A = (1/3)W_A$ and $R_A = (-2/3)W_A$. Solving the atmospheric response in equation (29) is akin to solving a matrix system $\mathbf{A}X = B$, where $X = \{W_{A_1}, \dots, W_{A_{n_A}}\}$. The zonal mean of E_q is removed in order to satisfy the solvability condition from equation (14), and the small dissipation $d_A = 10^{-8}$ ensures that the matrix \mathbf{A} is invertible without affecting solutions.

For numerical simulations, the system is further discretized in time with a timestep of 17h. We use a splitting method to update the system over each time step, where the deterministic model component is solved using an Euler method and the two-state Markov jump process is solved using a Gillespie algorithm (7). The initial conditions are an ocean at rest with a SST profile corresponding roughly to anomalies of 0.5 (-0.5) C in the eastern (western) Pacific (not shown).

5 Linear Solutions

In this section we analyze the linear solutions of the ENSO model. The leading mode in terms of growth/decay rate is a pair of oscillating eigenmodes, of the form $\underline{X} = \underline{A}\exp(-i\omega t)$, $\omega = \omega_r + i\omega_i$ with interannual frequency $\omega_r = \pm 0.22 \text{ yr}^{-1}$ (4.5 years oscillation period) and negative growth/decay rate $\omega_i = -0.5 \text{ yr}^{-1}$ (2 years decay period). This pair has the characteristics of the ENSO in nature, and is called hereafter the ENSO linear solution. The other linear solutions of the system are much more dissipated (with a growth/decay rate inferior to -4 yr^{-1}) and therefore are of lesser importance.

Figure S5 shows space-time hovmollers for the ENSO linear solution, $\underline{X} = \underline{A}\exp(-i\omega_r t)$ with the growth/decay ω_i omitted in the reconstruction. It consists of SST anomalies in the eastern Pacific, along with a tilted structure of thermocline anomalies and zonal currents in the central Pacific. Between El Niño and La Niña events, thermocline depth anomalies H are of same sign along the equator, which corresponds to a maximal/minimal heat content or warm water volume, as in nature.

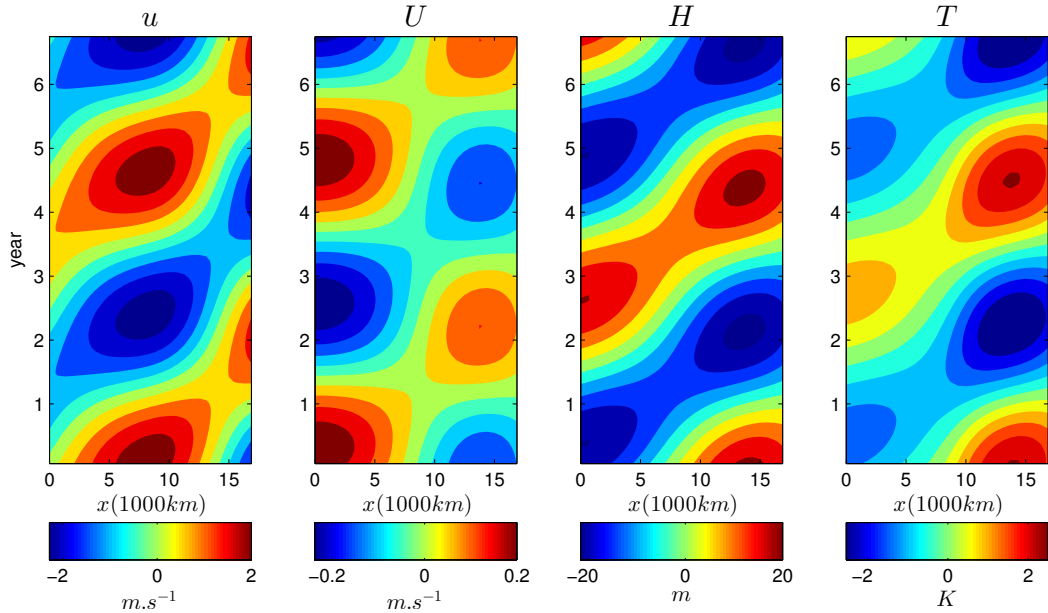


Figure S5: Hovmollers for the ENSO linear solution, variables at equator as a function of zonal position x (1000km) and time (years): winds u ($m.s^{-1}$), currents U ($m.s^{-1}$), thermocline depth H (m), and sea surface temperature T (K). Growth/Decay rate ω_i is omitted for the reconstruction.

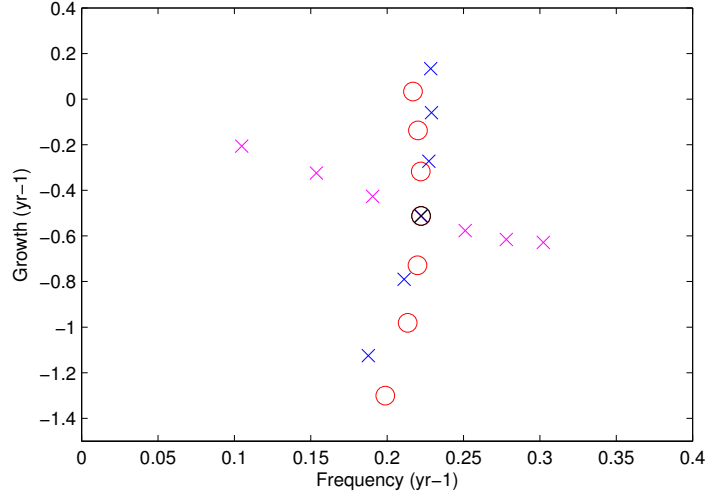


Figure S6: Scatterplot of Frequency ω_r (yr^{-1}) and Growth/Decay ω_i rate (yr^{-1}) for the ENSO linear solution. This is for solutions obtained with either reference parameter values (black circle and cross) or modified parameter values: ζ varied up to ± 1 of its reference value (red circles), γ varied up to ± 1 of its reference value (blue crosses), and α_q varied up to ± 0.15 of its reference value (purple crosses).

Figure S6 shows sensitivity of the ENSO linear solution to some parameter changes. Varying ζ or γ for example substantially modifies the growth/decay rate of the system, while varying α_q substantially modifies its frequency. Note in particular that ζ is the main source of dissipation in the model (although there are also dissipation losses due to reflections at ocean boundaries). There are obviously some uncertainty in the exact value of those parameter, as is usually the case in ENSO models, such that in practice values are chosen within a plausible range according to a desired model behavior.

The modified parameter values in Figure S6 could for example render the ENSO mode unstable (with positive growth rate). In such case, the ENSO cycle would have to be limited by system nonlinearities, for example reaching a limit cycle. In the present article, we rather assume that the ENSO linear solution is slightly dissipated, such that the ENSO cycle has to be maintained by wind burst activity.

References

- [1] A. J. Majda and S. N. Stechmann. The skeleton of tropical intraseasonal oscillations. *Proc. Natl. Acad. Sci.*, 106:8417–8422, 2009.
- [2] A. M. Moore and R. Kleeman. Stochastic Forcing of ENSO by the Intraseasonal Oscillation. *J. Climate*, 12:1199–1220, 1999.
- [3] A. J. Clarke. *An Introduction to the Dynamics of El Nino & the Southern Oscillation*. Academic Press, 2008.
- [4] S. Thual, O. Thual, and B. Dewitte. Absolute or convective instability in the equatorial pacific and implications for ENSO. *Q. J. Meteorol. Soc.*, 138, 2012.
- [5] A.J. Majda and R. Klein. Systematic multiscale models for the Tropics. *J. Atmos. Sci.*, 60:393–408, 2003.
- [6] S.N. Stechmann and H.R. Ogrosky. The walker circulation, diabatic heating, and outgoing longwave radiation. *Geophys. Res. Lett.*, 41:9097–9105, 2014.
- [7] A. J. Majda and J. Harlim. *Filtering Complex Turbulent Systems*. Cambridge University Press, 2012.